BIOCHEMISTRY
including biophysical chemistry & molecular biology

Article

pubs.acs.org/biochemistry

Domain Structure and Denaturation of a Dimeric Mip-like Peptidyl-Prolyl *cis–trans* Isomerase from *Escherichia coli*

Biswanath Jana,[†] Amitava Bandhu,[†] Rajkrishna Mondal,[†] Anindya Biswas,[†] Keya Sau,[‡] and Subrata Sau*[,†]

[†]Department of Biochemistry, Bose Institute, P-1/12, CIT Scheme VII M, Kolkata 700054, West Bengal, India

[‡]Department of Biotechnology, Haldia Institute of Technology, PO-HIT, Dt-Purba Medinipur, Pin 721657, West Bengal, India

Supporting Information

ABSTRACT: FKBP22, a protein expressed by *Escherichia coli*, possesses PPIase (peptidyl-prolyl *cis-trans* isomerase) activity, binds FK506 (an immunosuppressive drug), and shares homology with *Legionella* Mip (a virulence factor) and its related proteins. To understand the domain structure and the folding–unfolding mechanism of Mip-like proteins, we investigated a recombinant *E. coli* FKBP22 (His-FKBP22) as a model protein. Limited proteolysis indicated that His-FKBP22 harbors an N-terminal domain (NTD), a C-terminal domain (CTD), and a long flexible region linking the two domains. His-FKBP22, NTD$^+$ (NTD with the entire flexible region), and CTD$^+$ (CTD with a truncated flexible region) were unfolded by a two-state mechanism in the presence of urea. Urea induced the swelling of dimeric His-FKBP22 molecules at the pretransition state but dissociated it at the early transition state. In contrast, guanidine hydrochloride (GdnCl)-induced equilibrium unfolding of His-FKBP22 or NTD$^+$ and CTD$^+$ seemed to follow three-step and two-step mechanisms, respectively. Interestingly, the intermediate formed during the unfolding of His-FKBP22 with GdnCl was not a molten globule but was thought to be composed of the partially unfolded dimeric as well as various multimeric His-FKBP22 molecules. Dimeric His-FKBP22 did not dissociate gradually with increasing concentrations of GdnCl. Very low GdnCl concentrations also had little effect on the molecular dimensions of His-FKBP22. Unfolding with either denaturant was found to be reversible, as refolding of the unfolded His-FKBP22 completely, or nearly completely, restored the structure and function of the protein. Additionally, denaturation of His-FKBP22 appeared to begin at the CTD$^+$.

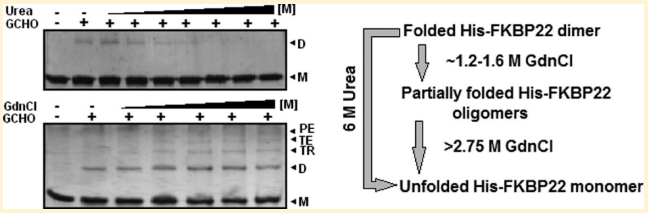

Escherichia coli expresses several different PPIase (peptidyl-prolyl *cis–trans* isomerase, EC 5.1.2.8) enzymes to ensure the proper folding of its nascent polypeptides.[1] Of the *E. coli* PPIases, FKBP22 possesses 206 amino acid residues and exists as a homodimer in solution.[2] The enzymatic activity of FKBP22 was inhibited by FK506 but not by cyclosporin A, both of which are immunosuppressive drugs. Interestingly, the amino acid sequence of FKBP22 was significantly identical with those of *Legionella pneumophila* Mip,[3] *Chlamydia trachomatis* Mip,[4] *Trypanosmoa cruzi* Mip,[5] *E. coli* FkpA,[6,7] *Salmonella typhimurium* FkpA,[8] *Shewanella* sp. FKBP22,[9] *Neisseria gonorrheae* Mip,[10] and *Xanthomonas campestris* Mip.[11] Mip (macrophage infectivity potentiator) proteins not only possess FKBP-type PPIase activity but also function as the virulence factors in pathogenic microorganisms. X-ray crystallography studies indicate that both *L. pneumophila* Mip[12] and *E. coli* FkpA[13] are homodimers with each monomer harboring two domains: an N-terminal domain and a C-terminal domain. While the N-terminal domain was suggested to be involved in protein dimerization, the C-terminal domain was predicted to contain the catalytic site for PPIase as well as the binding site for FK506. Biochemical studies have confirmed that the PPIase activity and FK506 or rapamycin binding site are in the C-terminal domain.[14−16] A putative N-terminal domain of *Shewanella* FKBP22 also exhibited dimerization in solution.[16] Interestingly, the domains are connected by an unusually long α-helix (termed α3) approximately 6.5 nm in length. Recently, a V-shaped structure, formed by the N-terminal domains of dimeric *Shewanella* FKBP22, was suggested to be critical for the PPIase activity with a protein substrate.[17] Additional studies indicate that *E. coli* FKBP22 is thermally more stable than *Shewanella* FKBP22.[16]

The way different nascent polypeptide chains fold and form the biologically active proteins is only partially understood.[18,19] Small, single-domain proteins are believed to fold by a reversible, two-state mechanism that comprises only the native and unfolded conformations. In contrast, oligomeric, multi-domain proteins seem to fold by multiple steps through the formation of one or more stable intermediates. Identification and characterization of the intermediate conformation are therefore crucial for understanding the mechanism of protein folding. One approach for identifying stable intermediates is the equilibrium unfolding of the protein with a chemical denaturant such as urea or GdnCl.[18,19] Using sensitive biophysical and biochemical probes, the structure, function, shape, and stability

Received: September 27, 2011
Revised: January 19, 2012
Published: January 20, 2012

   dx.doi.org/10.1021/bi2015037 | *Biochemistry* 2012, 51, 1223−1237

of various protein folding intermediates have been determined.[18−25]

Investigations of PPIase enzymes have revealed that unfolding pathways of these macromolecules can differ significantly.[21−25] While urea-induced unfolding of recombinant human FKBP12[21,22] followed a two-state mechanism, urea- and GdnCl-induced unfolding of *E. coli* trigger factor followed two-state and three-state mechanisms, respectively.[23,24] Interestingly, the urea-induced unfolding mechanism of a *Mycobacterium tuberculosis* cyclophilin (another PPIase) was altered from three-state to two-state in the presence of cyclosporin A.[25] Because of sequence homology, Mip proteins possessing PPIase activity possibly all form nonglobular, V-shaped, homodimeric structures in which two dumbbell-like monomers interact with each other at their N-terminal domains. Thus far, the folding−unfolding mechanism or the correlation between the dimeric state and the function of such PPIase enzymes has not been studied in the presence of chemical denaturants. Additionally, the two-domain structure of any Mip-like protein is yet to be supported by biochemical investigations. Using His-FKBP22 (a recombinant *E. coli* FKBP22) as the representative of Mip protein, here we have demonstrated that it is composed of two domains (NTD and CTD), which are connected by a long flexible region. We also show that urea-induced unfolding of His-FKBP22, NTD^+ (NTD with the flexible region), and CTD^+ (CTD with the truncated flexible region) followed a reversible two-state mechanism, whereas equilibrium unfolding of His-FKBP22 and NTD^+ occurred through the formation of various oligomeric intermediates in the presence of GdnCl. The properties of the oligomeric His-FKBP22 intermediates, however, did not match those of a true "molten globule".[26]

EXPERIMENTAL PROCEDURES

Materials. Urea, GdnCl (guanidine hydrochloride), glutaraldehyde, 8-anilino-1-naphthalenesulfonate (ANS), chymotrypsin, trypsin, thermolysin, acrylamide, bisacrylamide, PMSF (phenylmethanesulfonyl fluoride), FK506, juglone, cyclosporine, and IPTG (isopropyl β-D-1-thiogalactopyranoside) were purchased from Sigma, Merck, or SRL. Rapamycin was bought from BioVision. RNase T1 was bought from Fermentus. All other chemicals were of the highest purity available. The Ni-NTA resin and anti-His antibody were procured from Qiagen. The alkaline phosphatase-tagged goat anti-mouse antibody (IgG1-AP) was procured from Santa Cruz Biotechnology Inc. Restriction and modifying enzymes, Proofstart DNA polymerase, the plasmid isolation kit, the QIAquick gel extraction kit, the polymerase chain reaction (PCR) kit, oligonucleotides, protein, and DNA markers were obtained from Qiagen, Genetix Biotech Asia Pvt Ltd., and Hysel India Pvt Ltd. Benzamidine Sepharose resin was bought from GE Healthcare Biosciences Ltd.

Bacterial Strains, Plasmid, and Oligonucleotides. *E. coli* DH5α, *E. coli* BL21(DE3), and their derivatives were routinely cultivated in Luria-Bertani broth.[27] Growth medium was supplemented with IPTG and/or an appropriate antibiotic whenever needed.[27] Plasmid pET28a (Novagen) and *E. coli* strain BL21(DE3) were kind gifts of the late P. Roy (Bose Institute). Oligonucleotides P1 (5′CGGGATCCATGACCACCCCAACTTTTG), P2 (5′CCCAAGCTTTTAGAGGATTTCCAGCAG), N-f (5′CATGCCATGGGCACCACCCCAACTTTTGACAC), and N-b (5′CCGCTCGAGGTTTTCTTCCAGGTATTTCAC) were designed using the *fklB* gene sequence from *E. coli* K12 (National Center for Biotechnology Information, Bethesda, MD).

Basic DNA and Protein Techniques. Plasmid DNA isolation, DNA estimation, digestion of DNA by restriction enzymes, modification of DNA fragments by modifying enzymes, plasmid DNA transformation of *E. coli*, PCR, purification of DNA fragments, agarose gel electrophoresis, sodium dodecyl sulfate−polyacrylamide gel electrophoresis (SDS−PAGE), staining of polyacrylamide gels, and Western blotting were performed by the standard procedures[27−30] or according to the protocols provided by the respective manufacturers (Qiagen, Fermentas GmbH, and Bangalore Genei P. Ltd.). The total protein content was estimated by the Bradford assay using bovine serum albumin as the standard.[31]

Purification of His-FKBP22, NTD^+, and CTD^+. To purify *E. coli* FKBP22 as an N-terminal histidine-tagged variant (designated His-FKBP22), a 639 bp DNA fragment was amplified via PCR (using *E. coli* DH5α genomic DNA as the template and primers P1 and P2) and digested with *Bam*HI and *Hin*dIII followed by the cloning of the resulting fragment into pET28a, an *E. coli* expression vector. The insert of the derived vector (namely, p1280) was found to contain no mutation (evident from sequencing). Cloning has attached 34 additional amino acid residues (including a stretch of six His residues) at the N-terminal end of FKBP22. SAU1280 was generated by transforming p1280 into *E. coli* BL21(DE3). The crude extract, prepared from the IPTG-induced SAU1280 cells by a standard procedure,[30] was subjected to Ni-NTA column chromatography (Qiagen), and different fractions were collected according to the manufacturer's protocol. Analysis of the fractions described above by SDS−15% PAGE showed a single band of ∼25 kDa in the elution fraction (Figure S1A,B of the Supporting Information). This protein might be His-FKBP22 as its molecular mass matched the calculated molecular mass of His-FKBP22. The eluted protein was dialyzed against buffer B [20 mM Tris-HCl (pH 8.0), 300 mM NaCl, 1 mM EDTA, and 5% glycerol] or buffer C [100 mM phosphate buffer (pH 8.0), 300 mM NaCl, and 5% glycerol] for 12−16 h at 4 °C and stored on ice until it was used.

To purify CTD^+, nearly 500 μg of His-FKBP22 was digested with 5 μg of trypsin in 500 μL of buffer B for 16−18 h at 25 °C. The resulting peptide fragment-containing solution was incubated with 5 μL of benzamidine Sepharose resin (pre-equilibrated with buffer B) for 30 min at room temperature. After centrifugation, the nonparticulate fraction was collected and dialyzed against buffer B for 12−16 h at 4 °C. SDS−15% PAGE analysis of the dialyzed fraction showed primarily a single protein band of ∼14 kDa (Figure S1C of the Supporting Information). Sequencing and other analyses indicated it to be the CTD^+, which is composed of amino acid residues 77−206 of FKBP22 (Table 1 and Figures S1A and S2 of the Supporting Information).

To purify NTD^+, an amplification PCR was conducted using p1280 DNA as the template and primers N-f and N-b. The generated DNA fragment (290 bp) was digested with *Nco*I and *Xho*I followed by the cloning of the resulting DNA fragment into pET28a. The insert of the produced plasmid (designated p1303) did not bear any mutation (confirmed by DNA sequencing). SAU1303 was generated by transforming p1303 into *E. coli* BL21(DE3). The crude extract prepared from the IPTG-induced SAU1303 cells was treated and processed

Table 1. MALDI-TOF and Sequence Analyses of the Proteolytic Fragments

proteolytic fragment[a]	molecular mass of the fragment[b] (Da)	N-terminal end residues of the fragment[c]	possible FKBP22 region in the peptide fragment[d]
I	13942.432	QAMAA	Q112−L240
II	6971.992	–	G50−F111
IV	14090.442	FQAMA	F111−L240
V	7190	–	G18−K83
VI	7045.667	–	G33−R97
VIII	14091.239	–	F111−L240
IX	13743.099	MAAEG	M114−L240
X	6872.543	–	F40−A105

[a]Proteolytic fragments generated from His-FKBP22 are described in Figure 1. [b]Molecular masses of the proteolytic fragments were determined by MALDI-TOF analysis (see Experimental Procedures for details). [c]Five N-terminal end amino acid residues of fragments I, IV, and IX were determined by sequencing. [d]The molecular masses of the indicated regions of FKBP22 (estimated by Protparam on the ExPasy server) matched closely those determined by MALDI-TOF analysis. The FKBP22 fragments (II, V, VI, VIII, and X) therefore might be carrying the indicated regions mentioned above.

similarly as demonstrated for the purification of His-FKBP22 (see above). SDS−15% PAGE analysis of the eluted protein fraction primarily revealed a protein band of ∼11 kDa (Figure S1D of the Supporting Information). This protein might be NTD^+ (Figure S1A of the Supporting Information) as its molecular mass matched the molecular mass calculated from the primary sequence of NTD^+. NTD^+ harbors the first 91 amino acid residues of FKBP22 as well as nine other amino acid residues, including a histidine tag at the C-terminal end.

Activity of His-FKBP22 and CTD^+. To determine the PPIase activity of His-FKBP22, the RNase T1 (ribonuclease T1) refolding assay was performed mostly as described previously.[9] To study the inhibition of PPIase activity,[1] the RNase T1 refolding assay was also conducted in the presence of His-FKBP22, pre-equilibrated with different immunosuppressant drugs (e.g., cyclosporin A, juglone, and FK506).

To determine the K_d (equilibrium dissociation constant) value for the binding of rapamycin to His-FKBP22 and CTD^+, quenching of tryptophan fluorescence (λ_{ex} = 295 nm) of these proteins in the presence and absence of rapamycin was studied by a modified procedure.[32] Briefly, the tryptophan fluorescence intensity of 5 μM His-FKBP22 or CTD^+ aliquots (pre-equilibrated with 0−40 μM rapamycin) was measured at λ_{max} (330 nm for His-FKBP22 and 347 nm for CTD^+) using a Hitachi F-3000 spectrofluorimeter (bandwidth of 5 nm for both excitation and emission). The observed fluorescence intensities were corrected by subtracting the corresponding buffer fluorescence and by adjusting for inner filter effect[33] and volume changes. Finally, the K_d was determined by nonlinear fitting of the fluorescence data to the "one-site specific binding" equation (eq 1) using GraphPad Prism (GraphPad Software Inc.).

$$Y = (B_{max}[X])/(K_d + [X]) \quad (1)$$

where Y indicates the extent of fluorescence quenched at any rapamycin concentration ([X]), which was determined by subtracting the fluorescence in the presence of rapamycin from the fluorescence in the absence of rapamycin. B_{max} (i.e., maximal fluorescence quenched upon saturation of protein with rapamycin) was determined from the double-reciprocal plot of $1/Y$ versus $1/[X]$. The effect of methanol (used as a solvent for rapamycin) on fluorescence quenching was less than 2% under the assay conditions.

Identification of Domain(s) in His-FKBP22. To map the domain(s) in His-FKBP22, limited proteolysis of this recombinant protein was performed separately with trypsin, chymotrypsin, and thermolysin as described previously.[30] The resulting proteolytic fragments (particularly those are generated by digestion for 5−6 h) were processed as described previously.[34] The molecular masses of the fragments were determined by a MALDI-TOF instrument (Bruker Daltonics, Ettlingen, Germany) according to the manufacturer's protocol. The instrument was adjusted to determine the molecular masses of the fragments lying in the range of 6−20 kDa only. To confirm the cleavage sites, N-terminal ends of some stable peptide fragments of His-FKBP22 were also sequenced by a standard method (Applied Biosystems).

Spectroscopic Studies of the Urea- and GdnCl-Treated Proteins. All proteins in buffer B were treated with 0−7 M urea or 0−5 M GdnCl for 16−18 h at 4 °C before in vitro studies were performed. Aliquots of the freshly prepared stock solution of urea (10 M) or GdnCl (8 M) were always used for treatment. To study the effect of urea or GdnCl on the structures of His-FKBP22, NTD^+, and CTD^+, far-UV circular dichroism (CD) spectra (200−260 nm) and near-UV CD spectra (250−310 nm) of all protein aliquots (pretreated with or without denaturant) were recorded with a JASCO J815 spectropolarimeter essentially as described previously.[35] Protein concentrations were 10 μM for far-UV CD experiments and 15 μM for near-UV CD experiments.

To investigate the effects of denaturants on the tryptophan environment of His-FKBP22 and CTD^+, intrinsic tryptophan fluorescence spectra (λ_{em} = 300−400 nm, and λ_{ex} = 295 nm) of all urea- or GdnCl-treated protein (10 μM) aliquots were recorded with a Hitachi F-3000 spectrofluorimeter as described previously.[33,35] To understand the solvent accessibility of tryptophan residues during the unfolding of His-FKBP22 and CTD^+, acrylamide quenching of tryptophan fluorescence of urea- and GdnCl-treated His-FKBP22 and CTD^+ were studied.[35,36] All fluorescence intensity values, measured at the λ_{max} (λ_{ex} = 295 nm), were corrected by subtracting the corresponding buffer fluorescence and also by adjusting for inner filter effect[33] and volume changes. The acrylamide quenching data were analyzed with the Stern−Volmer equation.[33]

$$F_o/F = 1 + K_{sv}[Q] \quad (2)$$

where F_o, F, K_{sv}, and [Q] denote the fluorescence in the absence of acrylamide, the fluorescence in the presence of acrylamide, the Stern−Volmer constant, and the acrylamide concentration, respectively. From the slope of the plot of F_o/F versus [Q], K_{sv} was determined.

To determine the effect of GdnCl on the hydrophobic surface of His-FKBP22, the ANS fluorescence (λ_{ex} = 360 nm, and λ_{em} = 495 nm) of this protein (5 μM) was measured in the presence of 0−5 M GdnCl as described previously.[35] The concentration of ANS used in the study was 40 μM.

Refolding of Denatured Proteins. To study refolding, protein in buffer B was denatured with 7 M urea or 5 M GdnCl by a method similar to that described above. The unfolded protein was dialyzed against buffer B for 16−18 h at 4 °C followed by the recording of the far-UV CD spectrum of the sample as described above. Far-UV CD spectra of both

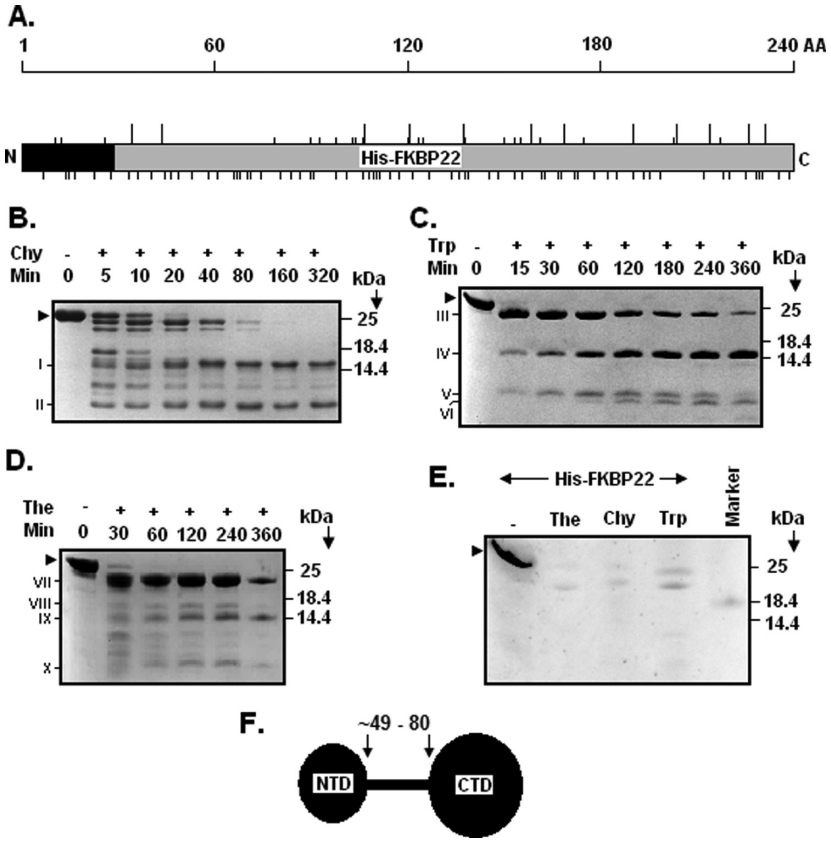

Figure 1. Limited proteolysis of His-FKBP22. (A) Schematic representation of N-terminally histidine-tagged *E. coli* FKBP22. The gray colored bar and the attached black bar indicate the *E. coli* FKBP22 and the additional 34 amino acid residues (including six His residues), respectively. The N-terminal end (N) and the C-terminal end (C) of His-FKBP22 are shown. A scale (in amino acid residues, AA) at the top of bar was drawn to describe the size of His-FKBP22. Trypsin and chymotrypsin cutting sites are denoted by small and long vertical lines immediately at the top of the bar, respectively. Thermolysin cleavage sites are shown by vertical lines at the bottom of the bar. Cleavage sites of all the enzymes mentioned above were identified by analyzing the primary sequence of His-FKBP22 using "PeptideCutter" from the ExPasy Web site. (B–D) Analyses of trypsin (Trp)-, chymotrypsin (Chy)-, and thermolysin (The)-digested His-FKBP22 fragments by SDS–13.5% PAGE. Masses (in kilodaltons) of marker proteins are shown at the right side of the gel. Different proteolytic fragments of His-FKBP22 are denoted by I–X. The arrowheads denote undigested His-FKBP22. (E) Western blotting analyses of the proteolytic fragments. The His-FKBP22 fragments from the 60 min trypsin, 60 min chymotrypsin, and 240 min thermolysin digestions were used in the study using an anti-His antibody. (F) Summary of limited proteolysis. As is evident from analysis of the proteolytic fragments (Table 1), a two-domain structure of the *E. coli* FKBP22 monomer harboring an N-terminal domain (NTD), a hinge region (encompassing amino acid residues ~49–80), and a C-terminal domain (CTD) is shown.

denatured and folded protein were also determined simultaneously for comparison. Protein concentrations were kept the same in all samples. To assess the refolding of domains of His-FKBP22, renatured His-FKBP22 (10 μM) in buffer B was digested with trypsin (at a protein:enzyme concentration ratio of 100:1) for different time periods followed by the analysis of the cleaved fragments by Tris-tricine SDS–13.5% PAGE. To check the function of refolded His-FKBP22, the RNase T1 refolding assay was performed using the same method described above.

Determination of the Oligomeric State and Shape of Proteins. To determine the oligomeric status of 2.5 μM His-FKBP22 or NTD$^+$ in the presence or absence of urea or GdnCl, a glutaraldehyde-mediated chemical cross-linking experiment was performed as described previously.[29] The intensity of each protein band elucidated via Tris-tricine SDS–13.5% PAGE was determined by a Versa Doc Imaging system (model 4000, Bio-Rad). To determine the molecular shape of His-FKBP22, NTD$^+$, and CTD$^+$ in the presence and absence of a denaturant, analytical gel filtration chromatography was performed using an ÄKTAprime Plus system (GE Healthcare Life Sciences) according to a standard method.[29,30]

Transverse Urea Gradient Gel. To probe the unfolding of His-FKBP22, NTD$^+$, and CTD$^+$ at the biochemical level, these macromolecules were also resolved separately through the transverse urea gradient gel (TUG) according to a standard procedure[37] with modifications. TUG with a 0 to 8 M linear urea gradient and a compensatory 10 to 7% acrylamide gradient was prepared using solutions I [10% acrylamide in 375 mM Tris-HCl (pH 8.5)] and II [7% acrylamide and 8 M urea in 375 mM Tris-HCl (pH 8.5)]. The acrylamide concentrations at 0 and 8 M urea were 10 and 7%, respectively. The polymerized gel was rotated 90° prior to the protein sample (usually 10–20 μg in buffer B and loading dye without SDS) being loaded on the single well at the top. Using 25 mM Tris-glycine buffer (pH 8.3) as a running buffer, gel electrophoresis was conducted at 65 V in the cold room (4 °C) for 4–8 h. The protein band in the gel was visualized by Coomassie Blue staining.

Analysis of Unfolding Curves. Assuming that unfolding of His-FKBP22, CTD$^+$, or NTD$^+$ follows a two-state model,[38] the fraction of unfolded protein molecules (f_u) was calculated from the following equation:

$$f_u = (X_n - X)/(X_n - X_u) \quad (3)$$

dx.doi.org/10.1021/bi2015037 | *Biochemistry* 2012, 51, 1223–1237

where X, X_n, and X_u represent the observed spectroscopic signal or mobility of the protein at any denaturant concentration, the spectroscopic signal or mobility of the protein in the completely folded state, and the spectroscopic signal or mobility of the protein in the completely unfolded state, respectively. From the straight lines (not shown) developed using the low and high denaturant concentrations of the unfolding curves, the values of X_n and X_u were determined.

C_m (denaturant concentration at the midpoint of unfolding transition) values of the two-state and three-state pathways were determined by nonlinear fitting of the unfolding data to eqs 4 and 5, respectively, using GraphPad Prism (GraphPad Software Inc.) as described previously.[39]

$$Y = \text{bottom} + (\text{top} - \text{bottom})/(1 + 10^{X-C_m}) \quad (4)$$

$$Y = \text{bottom} + (\text{bottom} + \text{top})F_1/(1 + 10^{X-C_{m1}}) + (\text{bottom} + \text{top})F_2/(1 + 10^{X-C_{m2}}) \quad (5)$$

where X, Y, F_1, and F_2 represent the concentration of unfolding agent, the fraction of unfolded protein molecules, the fraction of one kind of species, and the fraction of a second kind of species, respectively.

Statistical Analysis. All data are presented here as the means of at least three independent experiments with the standard deviation. Two data were considered significant if the corresponding p value (determined by a paired Student's t test) was found to be <0.05. Mean, standard deviation, and p values were determined with Microsoft Excel.

RESULTS AND DISCUSSION

Two-Domain Structure of His-FKBP22. The tertiary structure of *E. coli* FKBP22 should resemble those of *Legionella* Mip[12] and *E. coli* FkpA[13] as these proteins are significantly identical at the amino acid sequence level.[9] To get a glimpse of the structure of *E. coli* FKBP22, we developed a three-dimensional model structure of this protein by the standard procedures (see the Supporting Information for details). Figure S3 of the Supporting Information shows that the putative structure of *E. coli* FKBP22 is V-shaped and composed of two monomers like those of *L. pneumophila* Mip[12] and *E. coli* FkpA.[13] Each monomer carries two domains (CTD and NTD), which are connected by an extended α-helix (designated helix α3) consisting of 38 amino acid residues. While the NTD is composed of amino acid residues 1−54, the CTD harbors residues 93−206. The NTDs from two monomers are involved in dimerization, whereas the CTDs of the dimeric molecule possess PPIase substrate as well as drug (such as FK506 and rapamycin) binding sites.

The X-ray crystallographic and modeling data suggest that monomers of *Legionella* Mip and the related proteins possess a two-domain structure. No systematic biochemical experiment has been performed yet to confirm it conclusively. To resolve this issue, a recombinant *E. coli* FKBP22 (His-FKBP22) was purified as described previously (see Experimental Procedures and Figure S1A,B of the Supporting Information). His-FKBP22 exhibited PPIase activity that was inhibited by FK506 but not by cyclosporine A or juglone (Figure S1E of the Supporting Information). Besides, it interacted with the anti-His antibody, formed dimers in solution, and carried primarily α-helix (data not shown).

Limited proteolysis has long been used to study the domain structure in proteins.[40] To map the domain(s) in His-FKBP22, limited proteolysis of this protein was performed with three enzymes (e.g., chymotrypsin, trypsin, and thermolysin) separately (see Experimental Procedures for details). His-FKBP22 bears 12 chymotrypsin-specific, 21 trypsin-specific, and 67 thermolysin-specific cleavage sites at various locations (Figure 1A), indicating that a large number of peptide fragments could result from the digestion of His-FKBP22 by the proteinases mentioned above unless some of these sites are buried within the recombinant protein. Figure 1B shows the generation of two stable fragments (designated I and II) after the prolonged digestion of His-FKBP22 with chymotrypsin. In contrast, trypsinolysis of His-FKBP22 (Figure 1C) generated four distinct fragments (designated III−VI) with the molecular masses ranging from ∼24 to 6 kDa. While fragments III and V were degraded gradually, the intensity of fragment IV increased steadily with an increasing digestion time. Fragment VI appeared at the late stage of digestion. Like trypsin-mediated proteolysis, four major fragments (namely, VII−X) were also produced from the lysis of His-FKBP22 with thermolysin (Figure 1D). Of the fragments, fragment IX appeared to be relatively more stable than other fragments. None of the above fragments (I−X) reacted with the anti-His antibody, though the antibody did bind His-FKBP22 (Figure 1E). The data together indicate that His-FKBP22 harbors at least two highly enzyme accessible regions: one at the extreme N-terminal end and another somewhere in the middle of this protein. Fragments III and VII must have been generated by the removal of the N-terminal histidine tag as it carries several trypsin and thermolysin cleavage sites (Figure 1A). The remaining fragments were possibly produced by digestion within the internal region(s) of His-FKBP22.

To precisely map the proposed flexible region(s) in His-FKBP22, we performed MALDI-TOF analysis of the proteolytic peptide fragments mentioned above according to the standard procedure (see Experimental Procedures for details). Under the study conditions, the molecular masses of fragments I, II, IV, V, VI, VIII, IX, and X were determined to be 13942.432, 6791.992, 14090.442, 7190, 7045.667, 14091.239, 13743.099, and 6872.543 Da, respectively (Table 1). By comparing these molecular masses with the theoretical molecular masses of all the proteolytic fragments (generated by random cleavage at a single site or two sites), we suggest that fragments I, II, IV, V, VI, VIII, IX, and X are composed of amino acid residues Q112−L240, G50−F111, F111−240, G18−K83, G33−R97, F111−L240, M114−L240, and F40−A105, respectively. Sequencing did reveal that the five N-terminal end amino acid residues of fragments I, IV, and IX are QAMAA, FQAMA, and MAAEG, respectively (Table 1). The amino acid residues of fragments I, IV, and IX correspond to amino acid residues 112−116, 111−115, 114−118, respectively, of His-FKBP22. The data confirm that a His-FKBP22 monomer indeed harbors two flexible regions at different locations. While the flexible region at the extreme N-terminal end possesses amino acid residues ∼1−49 (corresponding to residues 1−17 of native FKBP22), the other putative flexible region is composed of residues ∼83−114 (equivalent to amino acid residues 49−80 of native FKBP22) of His-FKBP22. Of the 32 residues in the latter flexible region, 26 residues belong to the N-terminal end of helix α3 in FKBP22 (Figures S2 and S3 of the Supporting Information). The region carrying 11 C-terminal end residues (81−91) of helix α3 is probably not exposed as none of the four thermolysin cut sites in this region were actually cleaved by thermolysin (data not shown). The

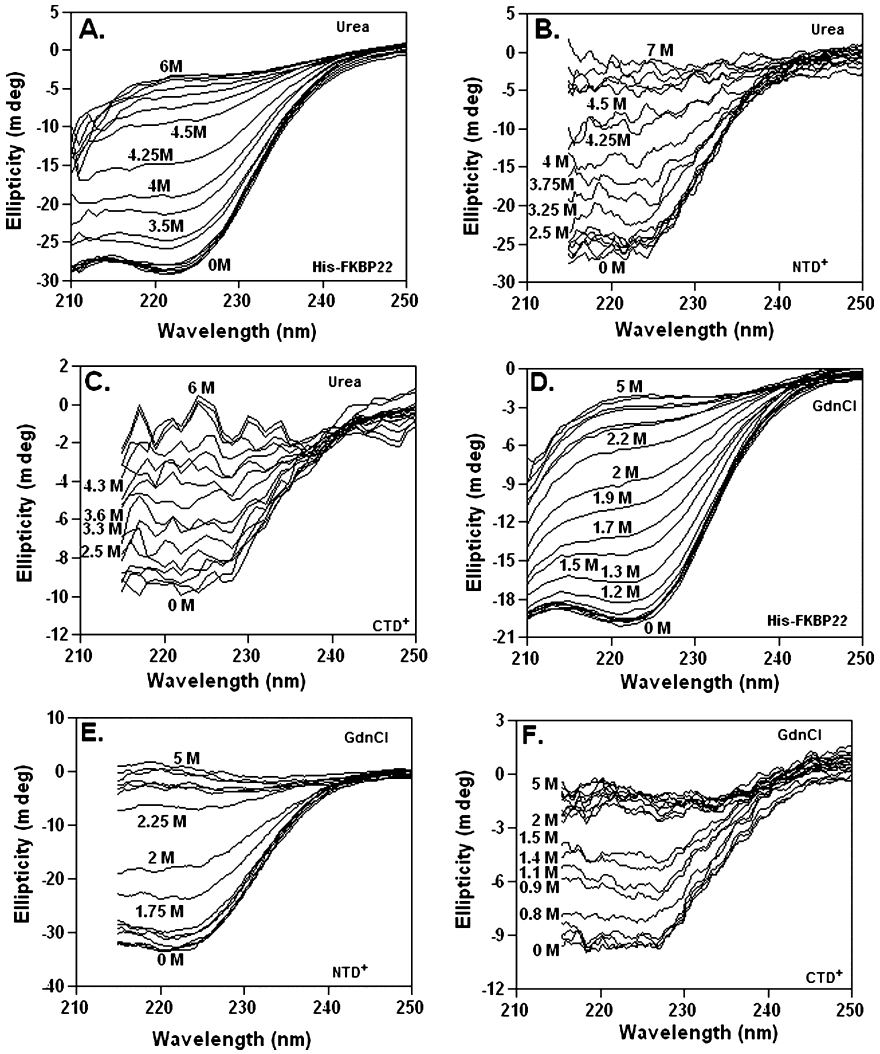

Figure 2. Effects of urea and GdnCl on the secondary structures of His-FKBP22 and its derivatives. Aliquots of His-FKBP22 (A and D), NTD$^+$ (B and E), and CTD$^+$ (C and F) were treated with 0−6 M urea (A−C) or 0−5 M GdnCl (D−F), and then their far-UV CD spectra were recorded at room temperature.

regions flanking the exposed regions are, therefore, highly folded and form roughly two domains (NTD and CTD) of FKBP22 (Figure 1F). While NTD that carries a small exposed region at its N-terminal end seems to carry amino acid residues ∼1−48, the CTD is composed of amino acid residues ∼81−206. Together, the data not only reveal the two-domain structure of FKBP22 but also suggest that the smaller NTD is more susceptible to proteolysis than the CTD. Because of less enzymatic stability, possibly NTD of *Legionella* Mip was not detected previously.[14]

In the absence of the helix α3-forming flexible region, the C-terminal domain of *Shewanella* FKBP22 exhibited no PPIase activity, whereas its N-terminal domain became unstable.[16,17] To study the unfolding of the CTD and NTD along with His-FKBP22, we purified two domain derivatives (CTD$^+$ and NTD$^+$) that carry either the truncated or the entire helix α3-forming flexible region (Figures S1A,C,D and S2 of the Supporting Information). CTD$^+$ bound to rapamycin with a K_d (equilibrium dissociation constant) value of 4.9 ± 0.7 μM, which is marginally lower than that determined for His-FKBP22 (Figure S1F of the Supporting Information). NTD$^+$ appeared to primarily carry α-helix (Figure S1G of the Supporting Information), interacted with the anti-His antibody, and formed homodimers in solution (data not shown).

Effect of Urea and GdnCl on the Secondary Structure of His-FKBP22 and Its Derivatives. The structure, function, and stability of a protein are usually altered upon it being exposed to any denaturant. To determine the effect of urea and GdnCl on the secondary structures of His-FKBP22, NTD$^+$, and CTD$^+$, we recorded the far-UV CD spectra of these proteins, pre-equilibrated individually with varying concentrations of urea and GdnCl (see Experimental Procedures for details). Figure 2A shows that the magnitudes of the peaks of the His-FKBP22-specific spectra at 222 nm were gradually decreased when urea concentrations were increased from ∼3 to 5 M. In contrast, the peaks of NTD$^+$-specific (Figure 2B) and CTD$^+$-specific (Figure 2C) spectra in ∼215−225 nm regions were reduced progressively at ∼2.5−5 M and ∼1.5−5 M urea, respectively. At urea concentrations of >5 M, none of the protein spectra possessed significant peaks at 222 nm or similar wavelengths. The peaks of the far-UV CD spectra of all three proteins at 222 nm and neighboring regions were found to be sensitive to GdnCl, as well (Figure 2D−F). The magnitudes of the peaks of the proteins were, however, reduced at much lower concentrations of GdnCl as GdnCl is a stronger denaturant

dx.doi.org/10.1021/bi2015037 | *Biochemistry* 2012, 51, 1223−1237

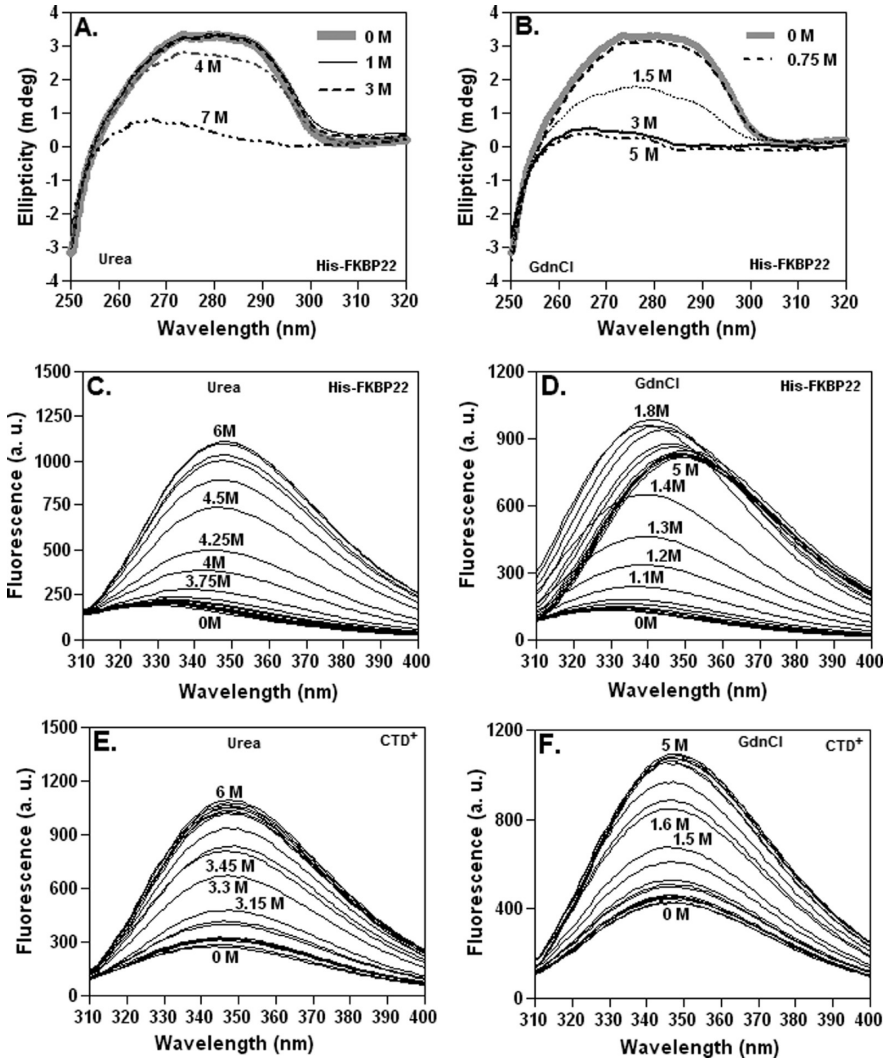

Figure 3. Effects of urea and GdnCl on the tertiary structures of His-FKBP22 and CTD$^+$. Near-UV CD spectra of His-FKBP22 in the presence of 0−7 M urea (A) and 0−5 M GdnCl (B). (C−F) Intrinsic Trp fluorescence spectra of His-FKBP22 (C and D) and CTD$^+$ (E and F) in the presence of varying concentrations of urea (C and E) or GdnCl (D and F).

than urea. While the magnitudes of the peaks of both His-FKBP22 and NTD$^+$ were decreased gradually when the GdnCl concentration was increased from ∼1 to 2.75 M, those of CTD$^+$ showed such reduction with ∼0.8−2 M GdnCl, indicating that the α-helix content of the latter protein decreases at relatively low GdnCl concentrations. The magnitudes of the peaks of His-FKBP22 and NTD$^+$ were not reduced considerably at ∼2.75−5 M GdnCl. Taken together, the data suggest that the α-helix content of His-FKBP22, NTD$^+$, and CTD$^+$ began decreasing at urea concentrations greater than ∼3, ∼2.5, and ∼1.5 M, respectively. Such stepwise reductions of the α-helix content of CTD$^+$ and His-FKBP22 or NTD$^+$ were achieved at GdnCl concentrations above ∼0.8 and ∼1 M, respectively. Because of unfolding, the α-helices in the proteins mentioned above were lost completely at urea concentrations of >5 M or at GdnCl concentrations above ∼2−2.75 M. The α-helix content of CTD$^+$ was affected more readily than those of the two other proteins in the presence of either denaturant.

Effect of Urea and GdnCl on the Tertiary Structures of His-FKBP22 and CTD$^+$. To determine the effect of urea and GdnCl on the tertiary structure of His-FKBP22, the near-UV CD spectra of the aliquots of this protein (pre-equilibrated separately with 0−7 M urea and 0−5 M GdnCl) were recorded as described in Experimental Procedures. In the absence of a denaturant, the near-UV CD spectrum showed a flattened peak of positive ellipticity around 268−288 nm (Figure 3A). The spectra of 1 and 3 M urea-equilibrated His-FKBP22 are nearly indistinguishable from that recorded at 0 M urea, whereas the peak of the spectrum of the 4 M urea-treated protein was reduced slightly. In contrast, a dramatic decrease in ellipticity was noticed in the spectrum of 7 M urea-treated His-FKBP22 (Figure 3A). Figure 3B shows that the near-UV CD spectrum of His-FKBP22 at 0.75 M GdnCl is nearly the same as that recorded at 0 M GdnCl. The size of the flattened peak with 1.5 M GdnCl (centered around 268−288 nm), however, decreased to approximately one-half of that monitored in the absence of GdnCl. In addition, the peak of the spectrum completely collapsed with 3 or 5 M GdnCl-treated His-FKBP22. Taken together, the tertiary structure of His-FKBP22 appeared to be perturbed when urea and GdnCl concentrations were made greater than 3 and 0.75 M, respectively.

The C-terminal domain of *E. coli* FKBP22 harbors two Trp residues at different positions.[2] Upon excitation at 295 nm, the intrinsic Trp fluorescence spectra of His-FKBP22 and CTD$^+$

dx.doi.org/10.1021/bi2015037 | *Biochemistry* 2012, 51, 1223−1237

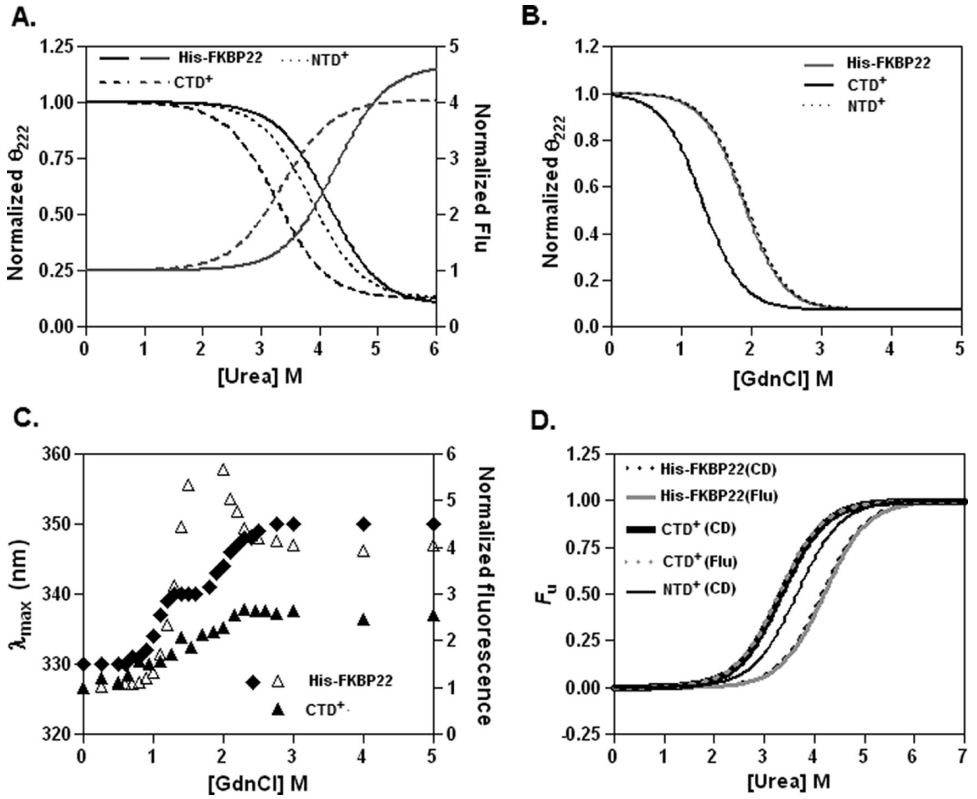

Figure 4. Mechanism of urea- and GdnCl-induced equilibrium unfolding of His-FKBP22 and its domain derivatives. (A) The θ_{222} (ellipticity at 222 nm) values, derived from the recorded far-UV CD spectra of a protein in the presence of urea (Figure 2A-C), were normalized with respect to that of the same protein in the absence of urea. The plots of normalized θ_{222} values vs urea concentrations indicate the alternation of secondary structure (particularly α-helix) of all three proteins at increasing urea concentrations. Similarly, intrinsic Trp fluorescence intensity values (Flu) at 330 nm (for His-FKBP22) and at 347 nm (for CTD) were determined from the fluorescence spectra (Figure 3B,C), normalized (as above), and plotted vs the corresponding urea concentrations. Fluorescence curves for His-FKBP22 and CTD$^+$ indicate the variation of tertiary structure of these proteins in the presence of increasing urea concentrations. The lines through the ellipticity or fluorescence values indicate best-fit curves. (B) Plots of the normalized θ_{222} (ellipticity) values vs GdnCl concentration show the unfolding of His-FKBP22, NTD$^+$, and CTD$^+$. The θ_{222} values derived from Figure 2D−F were normalized by the same procedure described above. The lines through the ellipticity values indicate the best-fit curves. (C) Plots showing the change in fluorescence intensity as well as λ_{max} values of His-FKBP22 and CTD$^+$ in the presence and absence of GdnCl. Both fluorescence values (at 330 nm for His-FKBP22 and 347 nm for CTD$^+$) and λ_{max} values were derived from panels E and F of Figure 3. (D) Fraction of unfolded protein (F_u) in the presence and absence of urea. F_u values were calculated from the far-UV circular dichroism (CD) and intrinsic Trp fluorescence (panel A) of His-FKBP22, NTD$^+$, and CTD$^+$ and plotted vs the respective urea concentrations by the standard procedures as described in Experimental Procedures.

exhibited emission maxima at 330 and 347 nm, respectively (data not shown). To determine whether the Trp environment in FKBP22 is sensitive to urea and GdnCl, intrinsic Trp fluorescence spectra of His-FKBP22 and CTD$^+$ (pre-equilibrated independently with 0−6 M urea and 0−5 M GdnCl) were recorded at room temperature (see Experimental Procedures for details). At ∼0−3 M urea, virtually no changes in either fluorescence or λ_{max} (wavelength of emission maxima) values were observed for His-FKBP22 (Figure 3C). The fluorescence intensities of His-FKBP22, however, tended to saturate at ∼5.5−6 M urea with λ_{max} values of 348−350 nm. Interestingly, the pattern of fluorescence spectra of His-FKBP22 at 0−5 M GdnCl (Figure 3D) appears to be different from that of His-FKBP22 recorded in 0−6 M urea (Figure 3C). There were 10 nm increments in the λ_{max} value when the GdnCl concentration was increased from ∼0.7 to 1.3 M. Thereafter, the λ_{max} values remained static at 340 nm until the GdnCl concentrations were made greater than 1.6 M. A further 10 nm red shift in λ_{max} was observed when the GdnCl concentration was increased to 2.75 M. The λ_{max} values remained fixed at 350 nm with 2.75−5 M GdnCl. As found with urea (Figure 3C), fluorescence intensity values gradually increased when GdnCl concentrations were increased from 0.75 to 1.8 M (Figure 3D). There was, however, stepwise quenching of the intensity values when GdnCl concentrations were further increased from ∼1.9 to 3 M. At GdnCl concentrations of >3 M, there was no additional alternation in the fluorescence intensity value. Conversely, fluorescence spectra of CTD$^+$ exhibited a gradual increase in the fluorescence intensity when urea and GdnCl concentrations were increased from ∼2 to 4 M (Figure 3E) and from ∼0.75 to 2.25 M (Figure 3F). At other denaturant concentrations, there was little change in the fluorescence intensity value. Throughout the unfolding process, the λ_{max} values of CTD remained fixed at 347 nm. Taken together, His-FKBP22 looks stable not only at 0−3 M urea but also at 0−0.75 M GdnCl. A urea or GdnCl concentration of >5 or >2.75 M, respectively, seemed to unfold this protein completely. Compared to His-FKBP22, initiation as well as the completion of the unfolding of CTD$^+$ appeared to occur at much lower denaturant concentrations. Interestingly, fluorescence intensity values of both His-FKBP22 and CTD$^+$ gradually increased during

dx.doi.org/10.1021/bi2015037 | *Biochemistry* 2012, 51, 1223−1237

unfolding (particularly at the beginning of their unfolding), indicating that there are considerable extents of fluorescence quenching in the folded state of these proteins. Various proteins, including a human FKBP, exhibited such quenching of Trp fluorescence at the native state.[21,41]

To precisely understand the effect of urea and GdnCl on the Trp accessibility of FKBP22, we have also investigated the quenching of Trp fluorescence of both His-FKBP22 and CTD^+ with acrylamide[36] in the presence and absence of both denaturants. The Stern−Volmer plots, derived from the quenching data of 0, 1, and 3 M urea-treated His-FKBP22, appeared to be very similar (Figure S4A of the Supporting Information) to the corresponding K_{sv} (Stern−Volmer constants) values ranging from 2.26 ± 0.15 to 2.31 ± 0.22 M^{-1} (Table S1 of the Supporting Information). The K_{sv} values also looked analogous when calculated from the quenching data of 0, 0.75, and 1.5 M GdnCl-treated His-FKBP22 (Figure S4B of the Supporting Information). At the denaturant concentrations that unfolded or partially unfolded His-FKBP22, the K_{sv} values were increased ∼2−4-fold, suggesting that two Trp residues of this protein become accessible to the aqueous solvent under these conditions. In contrast, the K_{sv} values were found to be nearly identical (Table S1 of the Supporting Information) when they were determined from the acrylamide quenching data of 0−5 M urea or GdnCl-treated CTD^+, indicating that two Trp residues in the native CTD^+ become exposed to the surface once the N-terminal domain is removed from His-FKBP22.

Mechanism of Urea- and GdnCl-Induced Unfolding. To obtain clues about the mechanism of urea- and GdnCl-induced unfolding of His-FKBP22 and its two domain derivatives, the negative ellipticity values of all these proteins at 222 nM were extracted from the far-UV CD spectra in Figure 2 and plotted versus the corresponding denaturant concentrations. All three proteins yielded sigmoidal curves with one transition in the presence of either denaturant (Figure 4A,B). All denaturation curves except those resulting from the GdnCl-induced unfolding of His-FKBP22 and NTD^+ showed transitions at distinct denaturant concentrations. The Trp fluorescence intensity values were also determined (from Figure 3C−F) and plotted versus the respective denaturant concentrations. All curves except that obtained from the GdnCl-induced unfolding of His-FKBP22 appeared to be roughly monophasic in nature (Figure 4A,C). The curve derived from the GdnCl-induced unfolding of His-FKBP22 was biphasic in nature with transition regions at ∼0.9−1.6 and ∼1.8−2.75 M GdnCl (Figure 4C). A biphasic curve also resulted when the associated λ_{max} values of His-FKBP22 (determined from Figure 3D) were plotted versus the corresponding GdnCl concentrations (Figure 4C). As Trp fluorescence spectroscopy is more sensitive than CD spectroscopy, we suggest that unfolding of His-FKBP22 in the presence of GdnCl follows a three-state mechanism with the formation of an intermediate. Conversely, urea-induced unfolding of all the proteins mentioned above and the GdnCl-induced unfolding of CTD^+ follow a two-step mechanism without the formation of any intermediate. To verify the predictions described above, the fraction of unfolded protein molecules, estimated from the far-UV CD (Figure 2) and the Trp fluorescence intensity data (Figure 3C,E,F) using eq 3, were plotted versus the respective denaturant concentrations. The resulting His-FKBP22- and CTD^+-specific unfolding curves (produced from the different urea-induced denaturation experiments) fit well to a two-state equation (eq 4) and were not only monophasic but also superimposable (Figure 4D). The NTD^+-specific curve derived from the urea-induced unfolding experiment also showed a monophasic pattern. The data together confirm that urea-induced unfolding of all three proteins occurs by the two-state mechanism without the formation of any stable intermediate. The CD data derived from the GdnCl-induced unfolding of all three proteins (Figure 4B) or the Trp fluorescence intensity data that resulted from the GdnCl-induced unfolding of CTD^+ (Figure 3D) also fitted nicely to the two-state equation (data not shown). The C_m (denaturant concentrations at the midpoint of unfolding transitions) values were determined from the fitted data described above and are presented in Table 2. The C_m value of CTD appeared to be significantly smaller than that of either His-FKBP22 or NTD^+, indicating that CTD^+ is the least stable of the three proteins. Previously, the thermal stability of the C-terminal domain of *Shewanella* FKBP22 was also found to be lower than that of its N-terminal domain.[9]

Table 2. C_m Values from Different Unfolding Assays[a]

protein	assay type	denaturant	C_{m1} (M)	C_{m2} (M)
His-FKBP22	far-UV CD	urea	4.16 ± 0.02	–
	Trp fluorescence	urea	4.19 ± 0.03	–
	TUGE	urea	4.68 ± 0.12	–
CTD^+	far-UV CD	urea	3.33 ± 0.03	–
	Trp fluorescence	urea	3.30 ± 0.04	–
	TUGE	urea	4.26 ± 0.09	–
NTD^+	far-UV CD	urea	3.64 ± 0.04	–
	TUGE	urea	4.64 ± 0.08	–
His-FKBP22	far-UV CD	GdnCl	1.88 ± 0.03	–
	Trp fluorescence	GdnCl	1.06 ± 0.16	1.97 ± 0.01
CTD+	far-UV CD	GdnCl	1.30 ± 0.04	–
	Trp fluorescence	GdnCl	1.39 ± 0.06	–
NTD^+	far-UV CD	GdnCl	1.88 ± 0.06	–

[a] C_m values were determined by fitting the equilibrium unfolding data (presented in Figures 4 and 5) to either eq 4 or 5. See the text for details.

The Trp fluorescence data obtained from the GdnCl-induced unfolding of His-FKBP22 (Figure 4C) fit well to a three-state equation (eq 5 and data not shown). The C_m values determined from the fitted plot of λ_{max} versus GdnCl concentration are 1.06 ± 0.16 and 1.97 ± 0.01, respectively (Table 2). The data indicate that GdnCl-induced unfolding of His-FKBP22, unlike the urea-induced unfolding of His-FKBP22, follows a three-state mechanism with the formation of an intermediate. The intermediate formed in the GdnCl-induced unfolding pathway of His-FKBP22 did not possess a substantial extent of secondary and tertiary structure (Figures 2D and 3D). An ANS binding experiment indicated that the amount of hydrophobic surface of His-FKBP22 was decreased in comparison with that of either the native or denatured form of this protein at 1.2−1.8 M GdnCl (data not shown). Such results are not supportive of the intermediate form being a true molten globule[26] that usually possesses an increased hydrophobic surface area and a substantial secondary structure but has a diminished level of tertiary structure. The intermediate form, therefore, may be merely a partially denatured form that

dx.doi.org/10.1021/bi2015037 | *Biochemistry* 2012, 51, 1223−1237

was produced from His-FKBP22 in the presence of moderate concentrations of GdnCl. A similar partially denatured intermediate was detected from the GdnCl-induced unfolding of a trigger factor possessing PPIase activity.[23]

Unfolding of His-FKBP22 and Its Domain Derivatives by a Biochemical Tool. Transverse urea gradient gel electrophoresis (TUGE), a popular biochemical method, has long been used to investigate the unfolding mechanism of proteins, the existence of folding intermediates, the dissociation and association of proteins (if multimeric in nature), the stability of homologous proteins, etc.[37,42] To confirm the unfolding mechanism of His-FKBP22, NTD$^+$, and CTD$^+$, the proteins were analyzed by TUGE following a standard procedure (see Experimental Procedures for details). The gels (Figure 5) showed that unfolding of all three proteins produced

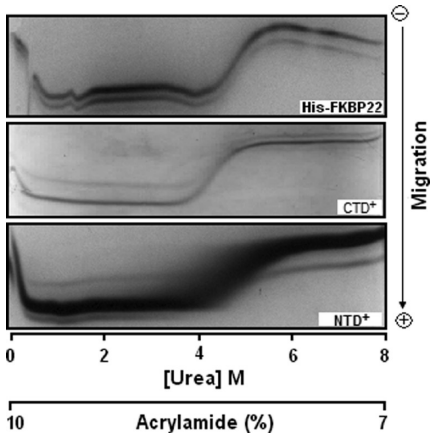

Figure 5. Mobility of His-FKBP22, NTD$^+$, and CTD$^+$ across the transverse urea gradient polyacrylamide gel.

what are primarily sigmoidal curve-like band patterns with one transition at ~4−5.5 M urea. All three proteins migrated roughly as linear bands at ~0.5−4 and ~5.5−8 M urea. Proteins at the latter urea concentrations, however, moved more slowly than those at the former urea concentrations. The relatively fast movements of all three proteins at very low urea concentrations (~0−0.5 M), which was probably due to the leakage of current along the edges of the gels,[43] were not considered in the analysis as secondary and tertiary structures of these proteins were not altered at 0−0.5 M urea (see above). In the transition regions, migrations of the proteins were slowed gradually as the concentration of unfolded molecules increased progressively with the increasing urea concentration. At ~5.5−8 M urea, all proteins mostly existed as the denatured forms. Such mobility patterns demonstrate that unfolding of His-FKBP22, NTD$^+$, and CTD$^+$ certainly follows the two-state mechanism with the formation of the denatured form directly from the native form. The C_m values for His-FKBP22, NTD$^+$, and CTD$^+$ were estimated from the TUGE data given above (see Experimental Procedures) and found to be 4.68 ± 0.12, 4.64 ± 0.08, and 4.26 ± 0.09, respectively (Table 2). The data again suggest that CTD$^+$ is a relatively unstable protein as the C_m value of this protein is significantly smaller than that of either His-FKBP22 (p = 0.023) or NTD$^+$ (p = 0.008).

Refolding of Unfolded His-FKBP22, NTD$^+$, and CTD$^+$. The urea- and GdnCl-induced denaturation of His-FKBP22, NTD$^+$, and CTD$^+$, if reversible in nature, would restore their native structures and function when denaturant will be withdrawn from the unfolding buffer. To verify this hypothesis, the far-UV CD spectra of native, likely refolded, and unfolded His-FKBP22, NTD$^+$, and CTD$^+$ were recorded (see Experimental Procedures for details). After renaturation of the urea-treated proteins, the CD spectra of all proteins were completely superimposed on those of respective native proteins (Figure 6A). In contrast, the CD spectrum of native His-FKBP22 did not completely coincide with that of renatured His-FKBP22 generated from the GdnCl-treated His-FKBP22 (Figure 6B). Dialyzing out GdnCl from the 5 M GdnCl-treated NTD$^+$ and CTD$^+$ samples, however, completely restored the secondary structure of His-FKBP22 derivatives (Figure 6A,B). Additional investigation revealed the superimposition of the Trp fluorescence spectrum of refolded His-FKBP22 (prepared from 7 M urea-treated His-FKBP22) on that of native His-FKBP22 (data not shown). Together, the data suggest the complete or nearly complete refolding of the proteins with the restoration of their structures.

To further test whether refolding of His-FKBP22 resulted in restoration of its two domains, both native His-FKBP22 and likely refolded His-FKBP22 were digested partially with trypsin followed by the resolution of the tryptic fragments by SDS−13% PAGE. As is evident from the gel pictures (Figure 6C,D), the molecular masses of all fragments from the refolded proteins (prepared from both 5 M GdnCl- and 7 M urea-treated His-FKBP22) were nearly identical to those generated by digestion of the native protein, indicating the proper refolding of the two domains, too.

To determine whether refolded His-FKBP22 possesses peptidyl-prolyl *cis-trans* isomerase activity, we performed the RNase T1 refolding assay as described here (see Experimental Procedures for details). Refolded His-FKBP22, prepared from either 7 M urea- or 5 M GdnCl-treated His-FKBP22, appeared to catalyze the refolding of RNase T1. The refolding activity of renatured His-FKBP22 was nearly identical to the activity of native His-FKBP22, when the PPIases were present at equimolar concentrations (Figure 6E,F). Restoration of the structure, domains, and enzymatic activity upon refolding thus proves the reversible nature of the unfolding pathways of all three proteins in the presence of urea and GdnCl.

Shape and Size of His-FKBP22 and Its Domain Derivatives in Urea and GdnCl Solutions. Our unfolding studies using urea and GdnCl (see above) could not clearly indicate whether the dimeric His-FKBP22 or NTD$^+$ molecules dissociated to stable monomers at the pretransition or transition state. To resolve the issue, we conducted glutaraldehyde-mediated cross-linking of these proteins, pre-equilibrated separately with 0−6 M urea and 0−2.5 M GdnCl (see Experimental Procedures). The top panel of Figure 7A shows that intensities of the dimer-specific bands of His-FKBP22 at 3−6 M urea are notably lower than those at 1−2 M urea. The intensities of the dimer-specific bands in Figure 7A were determined, normalized, and plotted versus the corresponding urea concentrations (Figure 7B). The resulting curve shows the decrease in the intensity of dimeric His-FKBP22 molecules from ~75 to 25% when urea concentrations were increased from 2 to 4 M. The midpoint of dimer dissociation was calculated to be 2.74 ± 0.22 M, indicating the dissociation of a majority of the dimeric molecules at urea concentrations above ~2.75 M. Unlike His-FKBP22, dimeric NTD$^+$ molecules appeared to be very stable at 3−4 M urea (bottom part of panel A of Figure 7A and panel B). The increased stability of dimeric NTD$^+$ at 3 or 4 M urea might be

dx.doi.org/10.1021/bi2015037 | *Biochemistry* 2012, 51, 1223−1237

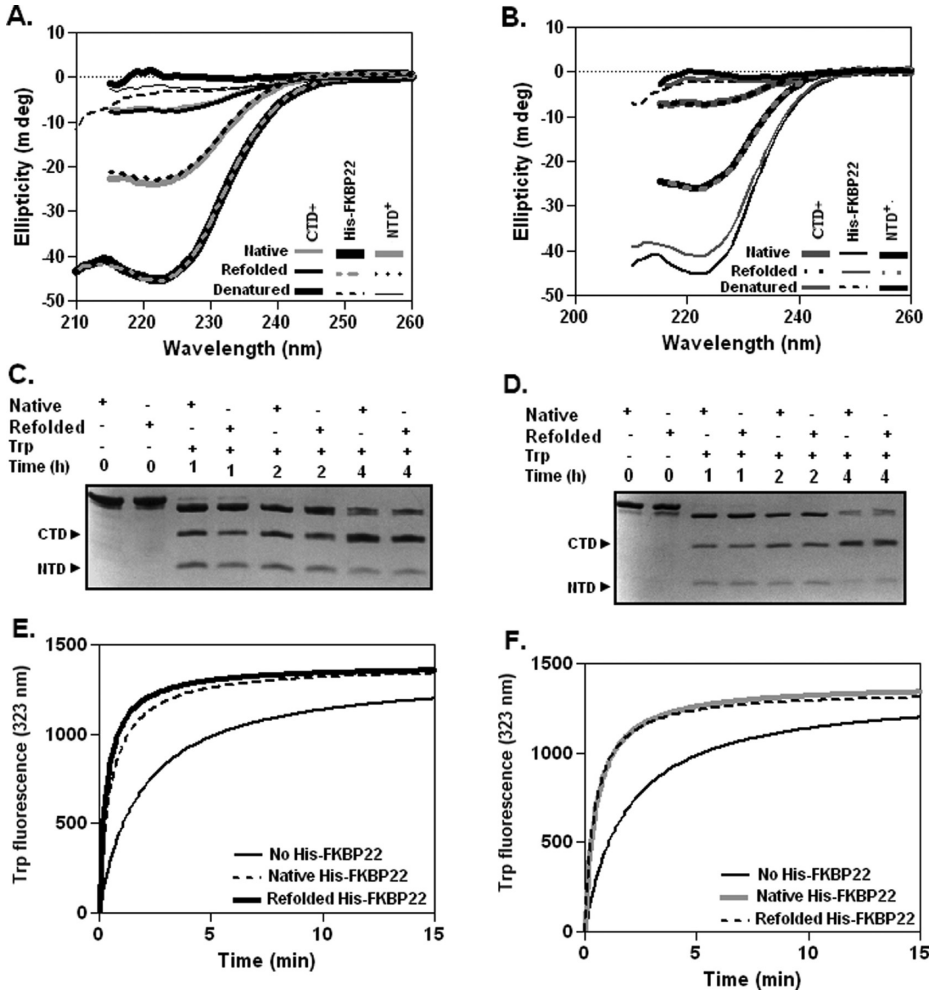

Figure 6. Refolding of denatured His-FKBP22, NTD$^+$, and CTD$^+$. Urea-denatured (A, C, and E) and GdnCl-denatured (B, D, and F) proteins were refolded followed by their analyses by various standard techniques. (A and B) Far-UV CD spectra of native, denatured, and refolded proteins at room temperature. (C and D) SDS−13.5% PAGE analysis of the peptide fragments generated from the digestion of native as well as refolded His-FKBP22 with trypsin (Trp). NTD and CTD are marked on the basis of the data presented in Figure 1C and Table 1. (E and F) RNase T1 refolding assay in the presence and absence of native and refolded His-FKBP22.

due to the exposure of an additional K residue (such as K86) besides K49. Contrary to the dissociation of dimeric His-FKBP22 by urea, dimeric His-FKBP22 remained mostly united in the presence of 0−2.5 M GdnCl (Figure 7C, left panel). Most notably, there was the formation of higher oligomeric forms (such as trimer, tetramer, pentamer, etc.) of His-FKBP22 in the presence of GdnCl. Synthesis of the higher oligomeric forms was enhanced at GdnCl concentrations above 0.5 M. The relative intensities of the higher oligomer-specific bands, however, appeared to be lower than that of the dimeric form. A cross-linking experiment also showed that NTD$^+$ did not undergo dissociation but formed various higher oligomeric forms in the presence of GdnCl (Figure 7C, right panel).

To improve our understanding of the effect of urea and GdnCl on the oligomeric status of His-FKBP22, we analyzed 0−6 M urea-equilibrated and 0−5 M GdnCl-equilibrated His-FKBP22 samples via gel filtration chromatography. The urea-treated (Figure 7D), GdnCl-treated (Figure 7E), and native His-FKBP22 samples all yielded a single peak with a distinct or nearly distinct retention volume. While the elution volume of native His-FKBP22 was 74.63 mL, 1, 3, 4, and 6 M urea-treated His-FKBP22 were eluted at 73.38, 70.63, 69.5, and 65.75 mL, respectively. The peak of 0.5 M GdnCl-treated His-FKBP22 nearly overlapped with that of native His-FKBP22. In contrast, 1, 1.25, and 3 M GdnCl-treated His-FKBP22 were eluted at 73, 71.63, and 67.38 mL, respectively. Compared to the elution profiles of some standard proteins (data not shown), the apparent molecular mass of the peak not treated with either urea or GdnCl corresponds to ∼64.4 kDa, which is ∼12 kDa higher than that estimated from the sequence of His-FKBP22. As reported for *Shewanella* FKBP22,[16] the relatively higher molecular mass of His-FKBP22 might be due to its nonglobular structure (Figure S3 of the Supporting Information). Currently, the apparent molecular masses related to the other peaks are not known with certainty. As noted above, the 0−6 M urea-treated NTD$^+$ and 0−5 M urea-treated CTD$^+$ samples also yielded a single peak with a unique elution volume (Figure S5 of the Supporting Information). While the retention volumes of NTD$^+$ samples at 0−6 M urea were decreased steadily from 74.5 to 63.37 mL, those of CTD$^+$ samples were reduced from 81.12 to 68.25 mL at 0−5 M urea. The early elution of the proteins in the presence of urea or GdnCl seems indicative of several molecular phenomena. At 6 M urea or 3 M GdnCl, complete unfolding of His-FKBP22 likely led to its elution prior to other samples. At 1−2 M urea, dimeric His-FKBP22 may have swelled to an extent that affected its elution. This

dx.doi.org/10.1021/bi2015037 | *Biochemistry* 2012, 51, 1223−1237

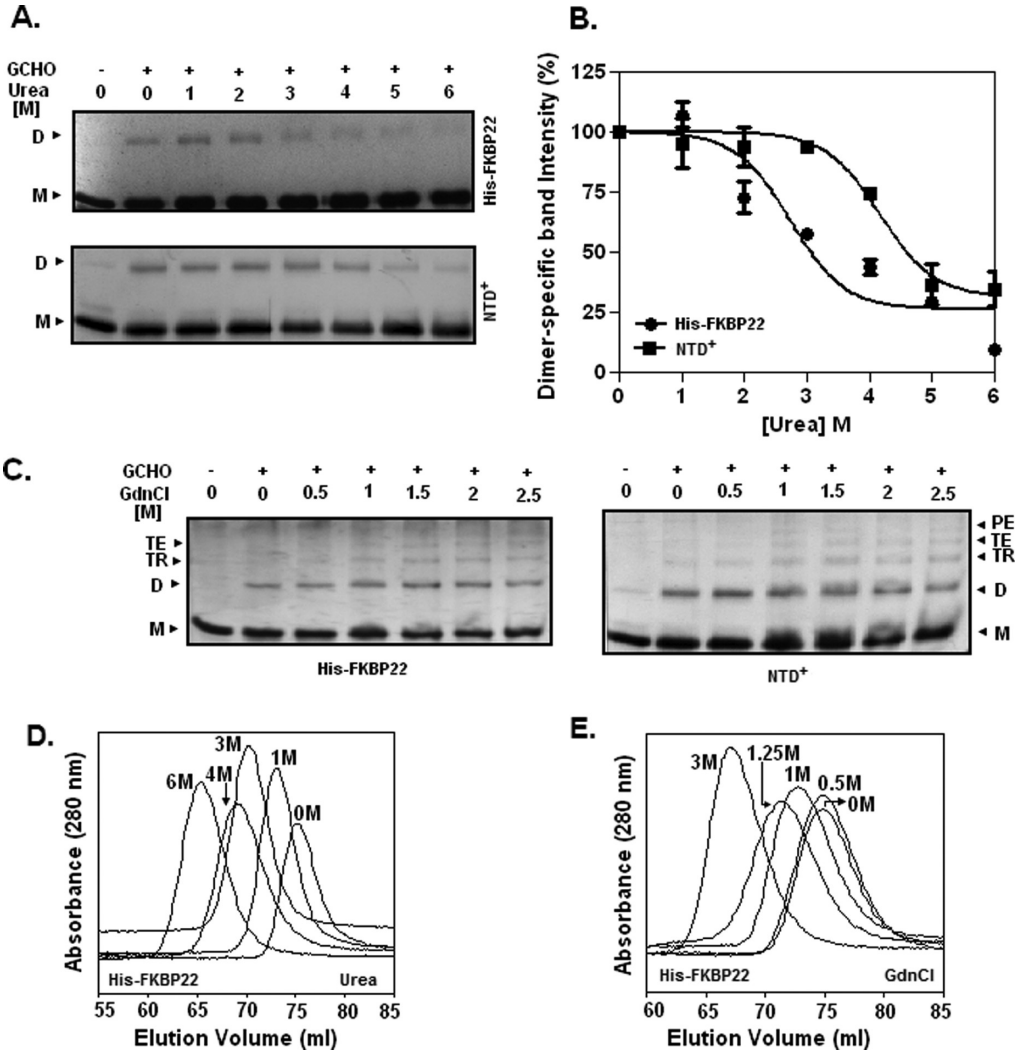

Figure 7. Determination of the molecular shape and oligomeric status of His-FKBP22, NTD$^+$, and CTD$^+$. (A) Chemical cross-linking of His-FKBP22 and NTD$^+$. Protein aliquots (pre-equilibrated with 0−6 M urea) were treated with 0.05% glutaraldehyde (GCHO) followed by their analysis using SDS−13.5% PAGE. Arrowheads denote dimer-specific (D) and monomer-specific (M) protein bands. (B) Plot of dimer-specific band intensity vs urea concentration. The intensity of a dimer-specific band (of His-FKBP22 or NTD$^+$) was normalized with respect to that of a monomer-specific band in the same lane of the SDS−PAGE images (A). Considering the normalized dimer-specific band intensity at 0 M urea as 100%, the normalized dimer-specific band intensities at other urea concentrations were determined. The error bars indicate standard deviations of three independent experiments. The solid lines through the band intensity values indicate the best-fit curves. (C) Chemical cross-linking of His-FKBP22 and NTD$^+$ (both pre-equilibrated with 0−5 M GdnCl) performed by a procedure similar to that described above. Arrowheads denote pentamer-specific (PE), tetramer-specific (TE), trimer-specific (TR), dimer-specific (D), and monomer-specific (M) protein bands. Masses (in kilodaltons) of marker proteins are shown at the right side of the gel. (D and E) Analytical gel filtration chromatography of His-FKBP22 in the presence of urea (D) and GdnCl (E). Protein peaks at a particular urea or GdnCl concentration are indicated. All protein samples (each at 20 μM) were injected onto a Superdex S-200 coulmn.

phenomenon has been observed with several other dimeric proteins that were not dissociated in the pretransition state.[44−46] For reasons not known, very low concentrations (e.g., 0.5 M) of GdnCl did not perturb the structure of His-FKBP22 and also did not swell this macromolecule.

His-FKBP22 that exists as a mixture of a dimer and a monomer at 3−4 M urea should be eluted at different times if these two forms are sufficiently stable. Two species, however, were little separated by the gel filtration chromatography described here. We rule out the complete unfolding of monomeric His-FKBP22 species as no additional peak corresponding to that of the 6 M urea-treated His-FKBP22 was seen at 3 or 4 M urea. Monomeric His-FKBP22 molecules most possibly were not aggregated as no extra peak was also noticed in the void volume region (data not shown). The single peak originated from 3 or 4 M urea-treated His-FKBP22, therefore, represents the average of its dimeric and monomeric forms, which are in the rapid equilibrium with each other. Support for this idea comes from the observation that the far-UV CD spectrum of refolded His-FKBP22 coincided with that of folded His-FKBP22 (Figure 4A). The lack of dimer- and monomer-specific peaks in the transition region, as we observed, is not an unprecedented event. Numerous other dimeric proteins exhibited a similar unified peak in the transition region.[46−48] The single peak that originated at 1 or 1.25 M GdnCl may also correspond to the average of all oligomers, which are in fast equilibrium in solution. We rule out this possibility as the far-UV CD spectrum of refolded His-

dx.doi.org/10.1021/bi2015037 | *Biochemistry* 2012, 51, 1223−1237

FKBP22 did not completely coincide with that of the equimolar concentration of native His-FKBP22 (Figure 6B). Alternatively, the single peak at 1 or 1.25 M GdnCl may represent dimeric His-FKBP22 as the higher-order oligomers, being less abundant in solution, may not be detected under the conditions of our gel filtration study.

Our biochemical and biophysical investigations indicate that GdnCl-induced unfolding of recombinant FKBP22 differs significantly from that of urea-induced unfolding. While urea-induced unfolding of His-FKBP22 follows a two-state mechanism, GdnCl-induced unfolding of this protein occurs through the formation of various intermediates (Figure 8). The

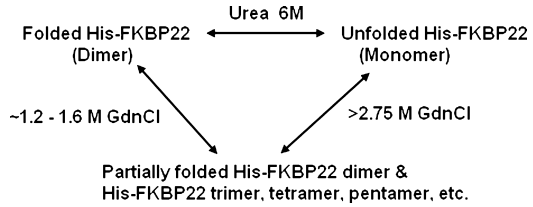

Figure 8. Schematic representation of urea- and GdnCl-induced unfolding of His-FKBP22.

unfolding pathway in the presence of either denaturant was, however, reversible in nature as there was complete or nearly complete restoration of the secondary structure, domain structure, and PPIase activity of His-FKBP22. At the pretransition state, urea caused swelling but did not affect the structure of His-FKBP22. In the presence of urea, dissociation of dimeric His-FKBP22 molecules was initiated in the early transition state and seemed to be completed before the completion of unfolding of the recombinant protein. In contrast, the molecular shape of His-FKBP22 remained mostly unaltered at very low GdnCl concentrations. Dissociation of dimeric His-FKBP22 was also not observed with increasing GdnCl concentrations. Our intrinsic Trp fluorescence data suggested the formation of an intermediate at ~1.2−1.6 M GdnCl (Figures 3E and 4D). We, however, could not identify an intermediate of the molten globule type.[26] Instead, it seems to be composed of a partially unfolded His-FKBP22 dimer and various higher-order oligomeric forms of His-FKBP22. The levels of synthesis of the higher-order oligomeric forms of His-FKBP22 were dramatically increased when GdnCl concentrations were ≥1 M. All forms of His-FKBP22 were unfolded at GdnCl concentrations above ~2.75 M.

In the presence of urea and GdnCl, unfolding of many proteins followed different mechanisms[23,24,49−51] even though the modes of action of these chaotropic agents are apparently similar.[52] The difference in the unfolding pathway was proposed to occur due to the generation of Gdn^+ and Cl^- from GdnCl in aqueous solution. Gdn^+, in particular, affects the structure of proteins by neutralizing the negatively charged amino acid residues involved in the formation of intramolecular ionic and hydrogen bonds in this macromolecule. It seems that Gdn^+-mediated partial unfolding of His-FKBP22 or NTD^+ exposed additional Lys residues, which in turn led to the formation of higher-order oligomeric forms of His-FKBP22 that were detected in the cross-linking experiment. It is not clear why the concentration of dimeric His-FKBP22 did not decrease gradually with an increasing GdnCl concentration.

CONCLUSIONS

This investigation has provided valuable information about the domain structure and the unfolding mechanism of *E. coli* FKBP22, a *Legionella* Mip-like peptidyl-prolyl *cis-trans* isomerase. Each FKBP22 monomer appears to harbor two domains (NTD and CTD) that are linked by a flexible region. In comparison with the CTD, the NTD is not only smaller but also more sensitive to the proteolytic enzymes. Urea-induced unfolding of a recombinant FKBP22, NTD^+, and CTD^+ indicates that all three proteins are denatured via a two-state mechanism without the formation of any intermediate. In contrast, GdnCl-induced unfolding of recombinant FKBP22 and NTD^+ seems to occur through the formation of various intermediates whose molecular properties were distinct from those of a molten globule. Unfolding of the CTD^+, however, follows a two-state mechanism in the presence of GdnCl. Additional investigations indicated that unfolding of recombinant FKBP22 with either denaturant is reversible in nature. Our unfolding studies also suggest that NTD^+ is more stable than CTD^+.

ASSOCIATED CONTENT

Supporting Information

Determination of Stern−Volmer constants (Table S1), purification and preliminary characterization of His-FKBP22, NTD^+, and CTD^+ (Figure S1), BLASTP analysis showing the alignment between *E. coli* FKBP22 and *L. pneumophila* Mip sequences (Figure S2), a three-dimensional model structure of *E. coli* FKBP22 (Figure S3), Stern−Volmer plots (Figure S4), and gel filtration chromatography of NTD^+ and CTD^+ in the presence of urea (Figure S5). This material is available free of charge via the Internet at http://pubs.acs.org.

AUTHOR INFORMATION

Corresponding Author

*E-mail: subratasau@gmail.com or subratasau@yahoo.co.in. Telephone: 91-33-2355-9416. Fax: 91-33-2355-3886.

Funding

The work was supported by grants from CSIR, Government of India [37(1427)/04/EMR-II], and BRNS/DAE, Government of India (2007/37/26/BRNS/1907), to S.S. B.J. received a Senior Research Fellowship from the Department of Atomic Energy (Government of India). A. Biswas is a recipient of a Junior Research Fellowship from the Council of Scientific and Industrial Research (Government of India).

Notes

The authors declare no competing financial interest.

ACKNOWLEDGMENTS

We are grateful to Dr. G. Chakrabarti (University of Calcutta, Calcutta, India) for his valuable suggestions during the work and for critically reading and rectifying the manuscript. We thank Dr. D. Cue who kindly corrected our revised manuscript. We also thank Mr. A. Banerjee, Mr. A. Poddar, Mr. J. Guin, and Mr. M. Das for their excellent technical support.

ABBREVIATIONS

PPIase, peptidyl-prolyl *cis-trans* isomerase; His-FKBP22, N-terminal histidine-tagged FKBP22 (a PPIase from *E. coli*); NTD, N-terminal domain of FKBP22; CTD, C-terminal domain of FKBP22; NTD^+, NTD harboring a long flexible region and nine additional amino acid residues; CTD^+, CTD

carrying a truncated flexible region at the N-terminal end; GdnCl, guanidine hydrochloride; MALDI-TOF, matrix-assisted laser desorption ionization time-of-flight.

REFERENCES

(1) Gothel, S. F., and Marahiel, M. A. (1999) Peptidyl-prolyl *cis-trans* isomerases, a superfamily of ubiquitous folding catalysts. *Cell. Mol. Life Sci. 55*, 423−436.

(2) Rahfeld, J. U., Rucknagel, K. P., Stoller, G., Horne, S. M., Schierhorn, A., Young, K. D., and Fischer, G. (1996) Isolation and amino acid sequence of a new 22-kDa FKBP-like peptidyl-prolyl *cis/trans*-isomerase of *Escherichia coli*. Similarity to Mip-like proteins of pathogenic bacteria. *J. Biol. Chem. 271*, 22130−22138.

(3) Engleberg, N. C., Carter, C., Weber, D. R., Cianciotto, N. P., and Eisenstein, B. I. (1989) DNA sequence of *mip*, a *Legionella pneumophila* gene associated with macrophage infectivity. *Infect. Immun. 57*, 1263−1270.

(4) Lundemose, A. G., Kay, J. E., and Pearce, J. H. (1993) *Chlamydia trachomatis* Mip-like protein has peptidyl-prolyl *cis/trans* isomerase activity that is inhibited by FK506 and rapamycin and is implicated in initiation of chlamydial infection. *Mol. Microbiol. 7*, 777−783.

(5) Moro, A., Ruiz-Cabello, F., Fernandez-Cano, A., Stock, R. P., and Gonzalez, A. (1995) Secretion by *Trypanosoma cruzi* of a peptidyl-prolyl *cis-trans* isomerase involved in cell infection. *EMBO J. 14*, 2483−2490.

(6) Horne, S. M., and Young, K. D. (1995) *Escherichia coli* and other species of the Enterobacteriaceae encode a protein similar to the family of Mip-like FK506-binding proteins. *Arch. Microbiol. 163*, 357−365.

(7) Ramm, K., and Pluckthun, A. (2000) The periplasmic *Escherichia coli* peptidylprolyl *cis,trans*-isomerase FkpA. II. Isomerase-independent chaperone activity in vitro. *J. Biol. Chem. 275*, 17106−17113.

(8) Horne, S. M., Kottom, T. J., Nolan, L. K., and Young, K. D. (1997) Decreased intracellular survival of an *fkpA* mutant of *Salmonella typhimurium* Copenhagen. *Infect. Immun. 65*, 806−810.

(9) Suzuki, Y., Haruki, M., Takano, K., Morikawa, M., and Kanaya, S. (2004) Possible involvement of an FKBP family member protein from a psychrotrophic bacterium *Shewanella* sp. SIB1 in cold-adaptation. *Eur. J. Biochem. 271*, 1372−1381.

(10) Leuzzi, R., Serino, L., Scarselli, M., Savino, S., Fontana, M. R., Monaci, E., Taddei, A., Fischer, G., Rappuoli, R., and Pizza, M. (2005) Ng-MIP, a surface-exposed lipoprotein of *Neisseria gonorrhoeae*, has a peptidyl-prolyl *cis/trans* isomerase (PPIase) activity and is involved in persistence in macrophages. *Mol. Microbiol. 58*, 669−681.

(11) Zang, N., Tang, D. J., Wei, M. L., He, Y. Q., Chen, B., Feng, J. X., Xu, J., Gan, Y. Q., Jiang, B. L., and Tang, J. L. (2007) Requirement of a *mip*-like gene for virulence in the phytopathogenic bacterium *Xanthomonas campestris* pv. campestris. *Mol. Plant-Microbe Interact. 20*, 21−30.

(12) Riboldi-Tunnicliffe, A., Konig, B., Jessen, S., Weiss, M. S., Rahfeld, J., Hacker, J., Fischer, G., and Hilgenfeld, R. (2001) Crystal structure of Mip, a prolylisomerase from *Legionella pneumophila*. *Nat. Struct. Biol. 8*, 779−783.

(13) Saul, F. A., Arie, J. P., Vulliez-le Normand, B., Kahn, R., Betton, J. M., and Bentley, G. A. (2004) Structural and functional studies of FkpA from *Escherichia coli*, a *cis/trans* peptidyl-prolyl isomerase with chaperone activity. *J. Mol. Biol. 335*, 595−608.

(14) Köhler, R., Fanghanel, J., Konig, B., Luneberg, E., Frosch, M., Rahfeld, J. U., Hilgenfeld, R., Fischer, G., Hacker, J., and Steinert, M. (2003) Biochemical and functional analyses of the Mip protein: Influence of the N-terminal half and of peptidylprolyl isomerase activity on the virulence of *Legionella pneumophila*. *Infect. Immun. 71*, 4389−4397.

(15) Ceymann, A., Horstmann, M., Ehses, P., Schweimer, K., Paschke, A., Michael Steinert, M., and Faber, C. (2008) Solution structure of the *Legionella pneumophila* Mip-rapamycin complex. *BMC Struct. Biol. 8*, 17.

(16) Suzuki, Y., Takano, K., and Kanaya, S. (2005) Stabilities and activities of the N- and C-domains of FKBP22 from a psychrotrophic bacterium overproduced in *Escherichia coli*. *FEBS J. 272*, 632−642.

(17) Budiman, C., Bando, K., Angkawidjaja, C., Koga, Y., Takano, K., and Kanaya, S. (2009) Engineering of monomeric FK506-binding protein 22 with peptidyl prolyl *cis-trans* isomerase. Importance of a V-shaped dimeric structure for binding to protein substrate. *FEBS J. 276*, 4091−4101.

(18) Jaenicke, R. (2000) Stability and stabilization of globular proteins in solution. *J. Biotechnol. 79*, 193−203.

(19) Kim, P. S., and Baldwin, R. L. (1990) Intermediates in the folding reactions of small proteins. *Annu. Rev. Biochem. 59*, 631−660.

(20) Neet, K. E., and Timm, D. E. (1994) Conformational stability of dimeric proteins: Quantitative studies by equilibrium denaturation. *Protein Sci. 3*, 2167−2174.

(21) Egan, D. A., Logan, T. M., Liang, H., Matayoshi, E., Fesik, S. W., and Holzman, T. F. (1993) Equilibrium denaturation of recombinant human FK binding protein in urea. *Biochemistry 32*, 1920−1927.

(22) Main, E. R., Fulton, K. F., and Jackson, S. E. (1999) Folding pathway of FKBP12 and characterisation of the transition state. *J. Mol. Biol. 291*, 429−444.

(23) Liu, C. P., Li, Z. Y., Huang, G. C., Perrett, S., and Zhou, J. M. (2005) Two distinct intermediates of trigger factor are populated during guanidine denaturation. *Biochimie 87*, 1023−1031.

(24) Zarnt, T., Tradler, T., Stoller, G., Scholz, C., Schmid, F. X., and Fischer, G. (1997) Modular structure of the trigger factor required for high activity in protein folding. *J. Mol. Biol. 271*, 827−837.

(25) Mitra, D., Mukherjee, S., and Das, A. K. (2006) Cyclosporin A binding to *Mycobacterium tuberculosis* peptidyl-prolyl *cis-trans* isomerase A: Investigation by CD, FTIR and fluorescence spectroscopy. *FEBS Lett. 580*, 6846−6860.

(26) Arai, M., and Kuwajima, K. (2000) Role of the molten globule state in protein folding. *Adv. Protein Chem. 53*, 209−282.

(27) Sambrook, J., and Russell, D. W. (2001) *Molecular cloning: A laboratory manual*, 3rd ed., Cold Spring Harbor Laboratory Press, Plainview, NY.

(28) Ausubel, F. M. (1987) *Current protocols in molecular biology*, Greene Publishing Associates and Wiley-Interscience, New York.

(29) Bandhu, A., Ganguly, T., Jana, B., Mondal, R., and Sau, S. (2010) Regions and residues of an asymmetric operator DNA interacting with the monomeric repressor of temperate mycobacteriophage L1. *Biochemistry 49*, 4235−4243.

(30) Ganguly, T., Das, M., Bandhu, A., Chanda, P. K., Jana, B., Mondal, R., and Sau, S. (2009) Physicochemical properties and distinct DNA binding capacity of the repressor of temperate *Staphylococcus aureus* phage ϕ11. *FEBS J. 276*, 1975−1985.

(31) Bradford, M. M. (1976) A rapid and sensitive method for the quantitation of microgram quantities of protein utilizing the principle of protein-dye binding. *Anal. Biochem. 72*, 248−254.

(32) Wear, M. A., Patterson, A., and Walkinshaw, M. D. (2007) A kinetically trapped intermediate of FK506 binding protein forms in vitro: Chaperone machinery dominates protein folding in vivo. *Protein Expression Purif. 51*, 80−95.

(33) Lakowicz, J. R. (1999) *Principles of fluorescence spectroscopy*, 2nd ed., Kluwer Academic/Plenum, New York.

(34) Wessel, D., and Flugge, U. I. (1984) A method for the quantitative recovery of protein in dilute solution in the presence of detergents and lipids. *Anal. Biochem. 138*, 141−143.

(35) Creighton, T. E. (1997) *Protein Structure: A Practical Approach*, 2nd ed., IRL Press at Oxford University Press, New York.

(36) Eftink, M. R., and Ghiron, C. A. (1981) Fluorescence quenching studies with proteins. *Anal. Biochem. 114*, 199−227.

(37) Goldenberg, D. P., and Creighton, T. E. (1984) Gel electrophoresis in studies of protein conformation and folding. *Anal. Biochem. 138*, 1−18.

(38) Pace, C. N., and Shaw, K. L. (2000) Linear extrapolation method of analyzing solvent denaturation curves. *Proteins Suppl. 4*, 1−7.

(39) Chakrabarty, S. P., and Balaram, H. (2010) Reversible binding of zinc in *Plasmodium falciparum* Sir2: Structure and activity of the apoenzyme. *Biochim. Biophys. Acta 1804*, 1743−1750.
(40) Fontana, A., de Laureto, P. P., Spolaore, B., Frare, E., Picotti, P., and Zambonin, M. (2004) Probing protein structure by limited proteolysis. *Acta Biochim. Pol. 51*, 299−321.
(41) Royer, C. A., Mann, C. J., and Matthews, C. R. (1993) Resolution of the fluorescence equilibrium unfolding profile of trp aporepressor using single tryptophan mutants. *Protein Sci. 2*, 1844−1852.
(42) Gianazza, E., Miller, I., Eberini, I., and Castiglioni, S. (1999) Low-tech electrophoresis, small but beautiful, and effective: Electrophoretic titration curves of proteins. *Electrophoresis 20*, 1325−1338.
(43) Siddiqui, K. S., Feller, G., D'Amico, S., Gerday, C., Giaquinto, L., and Cavicchioli, R. (2005) The active site is the least stable structure in the unfolding pathway of a multidomain cold-adpated amylase. *J. Bacteriol. 187*, 6197−6205.
(44) Park, C. Y., and Bedouelle, H. (1998) Dimeric tyrosyl-tRNA synthetase from *Bacillus stearothermophilus* unfolds through a monomeric intermediate. *J. Biol. Chem. 273*, 18052−18059.
(45) Agarwalla, A., Gokhale, R. S., Santi, D. V., and Balaram, P. (1996) Covalent tethering of the dimer interface annuls aggregation in thymidylate synthase. *Protein Sci. 5*, 270−277.
(46) Cellini, B., Bertoldi, M., Montioli, R., Laurents, D. V., Paiardini, A., and Voltattorni, C. B. (2006) Dimerization and folding processes of *Treponema denticola* cystalysin: The role of pyridoxal 5′-phosphate. *Biochemistry 45*, 14140−14154.
(47) Kim, D. H., Nam, G. H., Jang, D. S., Yun, S., Choi, G., Lee, H. C., and Choi, K. Y. (2001) Roles of dimerization in folding and stability of ketosteroid isomerase from *Pseudomonas putida* biotype B. *Protein Sci. 10*, 741−752.
(48) Najera, H., Costas, M., and Fernandez-Velasco, D. A. (2003) Thermodynamic characterization of yeast triosephosphate isomerase refolding: Insights into the interplay between function and stability as reasons for the oligomeric nature of the enzyme. *Biochem. J. 370*, 785−792.
(49) Akhtar, M. S., Ahmad, A., and Bhakuni, V. (2002) Guanidinium chloride- and urea-induced unfolding of the dimeric enzyme glucose oxidase. *Biochemistry 41*, 3819−3827.
(50) Rashid, F., Sharma, S., and Bano, B. (2005) Comparison of guanidine hydrochloride (GdnHCl) and urea denaturation on inactivation and unfolding of human placental cystatin (HPC). *Protein J. 24*, 283−292.
(51) Singh, A. R., Joshi, S., Arya, R., Kayastha, A. M., and Saxena, J. K. (2010) Guanidine hydrochloride and urea-induced unfolding of *Brugia malayi* hexokinase. *Eur. Biophys. J. 39*, 289−297.
(52) Nandi, P. K., and Robinson, D. R. (1984) Effects of urea and guanidine hydrochloride on peptide and non-polar groups. *Biochemistry 23*, 6661−6668.